

Titre: A new algorithm and system for the extraction of delta-lognormal parameters
Title:

Auteurs: Moussa Djioua, & Réjean Plamondon
Authors:

Date: 2008

Type: Rapport / Report

Référence: Djioua, M., & Plamondon, R. (2008). A new algorithm and system for the extraction of delta-lognormal parameters. (Rapport technique n° EPM-RT-2008-04). <https://publications.polymtl.ca/3165/>
Citation:

 **Document en libre accès dans PolyPublie**
Open Access document in PolyPublie

URL de PolyPublie: <https://publications.polymtl.ca/3165/>
PolyPublie URL:

Version: Version officielle de l'éditeur / Published version

Conditions d'utilisation: Tous droits réservés / All rights reserved
Terms of Use:

 **Document publié chez l'éditeur officiel**
Document issued by the official publisher

Institution: École Polytechnique de Montréal

Numéro de rapport: EPM-RT-2008-04
Report number:

URL officiel:
Official URL:

Mention légale:
Legal notice:

EPM-RT-2008-04

**A NEW ALGORITHM AND SYSTEM FOR THE
EXTRACTION OF DELTA-LOGNORMAL PARAMETERS**

Moussa Djoua et Réjean Plamondon
Département de Génie électrique
Laboratoire Scribens
École Polytechnique de Montréal

Mai 2008

Poly

EPM-RT-2008-04

A New Algorithm and System for the Extraction of Delta-Lognormal Parameters

Moussa DJIOUA et Réjean PLAMONDON

Département de Génie Électrique,
Laboratoire Scribens,
École Polytechnique de Montréal.

05/2008

©2008
Moussa Djioua, Réjean Plamondon
Tous droits réservés

Dépôt légal :
Bibliothèque nationale du Québec, 2008
Bibliothèque nationale du Canada, 2008

EPM-RT-2008-04

A New Algorithm and System for the Extraction of Delta-Lognormal Parameters

: Moussa Djioua, Réjean Plamondon
Département de génie électrique, Laboratoire Scribens
École Polytechnique de Montréal

Toute reproduction de ce document à des fins d'étude personnelle ou de recherche est autorisée à la condition que la citation ci-dessus y soit mentionnée.

Tout autre usage doit faire l'objet d'une autorisation écrite des auteurs. Les demandes peuvent être adressées directement aux auteurs (consulter le bottin sur le site <http://www.polymtl.ca/>) ou par l'entremise de la Bibliothèque :

École Polytechnique de Montréal
Bibliothèque – Service de fourniture de documents
Case postale 6079, Succursale «Centre-Ville»
Montréal (Québec)
Canada H3C 3A7

Téléphone : (514) 340-4846
Télécopie : (514) 340-4026
Courrier électronique : biblio.sfd@courriel.polymtl.ca

Ce rapport technique peut-être repéré par auteur et par titre dans le catalogue de la Bibliothèque :
<http://www.polymtl.ca/biblio/catalogue/>

Abstract—In this report, we present a new analytical method to estimate the parameters of Delta-lognormal functions. According to the Kinematic Theory of rapid human movements, these parameters contain information both on the motor commands and on the timing properties of a neuromuscular system. The new algorithm, called XZERO, exploits relationships between the zero crossings of the first and the second time-derivatives of a lognormal function and its four basic parameters. The methodology is described and evaluated in various testing conditions. Furthermore, for the first time, the extraction accuracy is quantified empirically, taking advantage of the exponential relationships that link the dispersion of the extraction errors with its signal to noise ratio. A new extraction system, which uses a benchmark of three estimation methods, is also proposed and evaluated in the mid-term perspective of developing machine intelligence applications that rely on lognormal functions.

Index Terms— Pattern recognition, Kinematic Theory, rapid movement, Delta-Lognormal model, lognormal function, parameter extraction, motor control, nonlinear regression, optimization, curve fitting.



1 INTRODUCTION

IN pattern analysis and recognition of on-line handwriting, various methods use a discontinuous representation scheme to represent a complex pattern, like a graph, a letter, a word, a signature, etc., with the superimposition of handwriting strokes, considered as a specific class of rapid human movements [1],[2],[3],[4],[5]. In motor control, these strokes are considered as primitives from which, complex movements are build

[6],[7],[8],[9],[10], [11],[12]. Thus, handwriting strokes have been intensively used and studied in many fields of research.

For example, in the forensic sciences, a detailed study of individual stroke patterns, focusing on tiny variations, often constitutes the grounds for a decision about the authenticity of a signature or a document [13],[14]. In education, various interactive teaching methods have been developed to reproduce letters and words from the concatenation of neat strokes [15], [16]. In the neurosciences, strokes are analyzed to both characterize neurodegenerative processes like Parkinson's and Alzheimer's diseases [17],[18] and, to evaluate the recovery processes in the rehabilitation of patients from cerebrovascular accidents [19]. In anthropomorphic robotics, the superimposition of handwriting strokes is used to explore the biomechanical principles employed by humans to produce movements and later to apply them in the control of a robot arm [20].

Many of these examples suggest that for a realistic analysis and understanding of how the motor control system performs complex movements, one should study the basic properties of single strokes. Running such a study for a specific application, one could then use a segmentation/superimposition strategy to construct an efficient machine intelligent system, which could globally processes complex movements to design for example an online handwriting recognition system [1]. The cornerstone of this whole methodology is then to understand, in the first place, the stroke genesis, since it reflects some fundamental properties of the neuromuscular system of a writer, as well as some basic features of the motor control strategies that are used to produce a simple movement. In this perspective, many studies have been conducted to understand the emergence of a basic pattern: the stereotyped bell-shaped velocity profile of these basic primitives [21],[22],[23],[24]. Among the various

computational models and theories developed to model this phenomenon, the Kinematic Theory [25] exploits an analytical expression, a Delta-Lognormal function, which takes into account the behavior of agonist and antagonist lognormal neuromuscular systems, specified by four system parameters, and describes the effective motor control of a movement by three command parameters. So far, many applications based on this theory have been developed [26],[27],[28],[35]. However, in term of fully automatic pattern analysis, the quest for an efficient software tool (an extraction system), which accurately estimates the seven parameters such that a velocity profile can be fitted with a Delta-Lognormal equation with a minimum reconstruction error remains an open problem. Consequently, various methods have been proposed to track this task, leading to three main categories of approaches: statistical, deterministic and evolutionary. Statistical methods rely on parameter estimation algorithms that deal with lognormal random variable densities [29], [30]. Deterministic methods focus on specific points on the velocity curve to first estimate the parameters and then use optimization algorithms to converge on optimal solutions [31],[32]. Evolutionary methods, using for example breeder genetic algorithms, have also been implemented [33], [34], [35].

Moreover, comparative studies have shown that the deterministic methods were more efficient than the statistical [27] and the evolutionary ones [33],[34]. So far, two deterministic approaches have lead to successful applications dealing with the analysis-by-synthesis of handwriting and signature verification [26],[27],[28],[31],[35], as well as the quantification of the performances of the Delta-Lognormal model with more than 26 other kinematic models [36],[37],[38],[39]. However, some studies have shown that these deterministic algorithms fail especially when the antagonist component is preponderant before the agonist component and when important noise is present in the signal [32],[40].

In this paper, we propose a new analytical algorithm developed to compensate for these various failures, to improve the performances of the existing extraction system, and to enlarge the range of Delta-Lognormal profiles that can be processed automatically. In summary, the new algorithm exploits analytical expressions that link the zero crossing of the first and the second time-derivatives of a lognormal function to its parameters. Furthermore, this study includes a methodology to quantify the accuracy of the extraction results under noise constraints by constructing a confidence interval for each extracted parameter value.

The remaining of the paper is organized as follows: In section 2, an overview of the Kinematic Theory and its Delta-Lognormal model is presented, while the architecture of the extraction system is depicted in Section 3. The new XZERO algorithm is described in details in Section 4. The performance results obtained in ideal and noisy conditions are presented and discussed in Section 5. In Section 6, a complete extraction system is proposed and the methodology used to quantify its accuracy is developed. Typical examples involving real data are presented in section 7 to highlight the power of the upgraded Delta-Lognormal extraction system.

2 OVERVIEW OF THE DELTA-LOGNORMAL MODEL

Among the various models used to study rapid movements, the Delta-Lognormal model has been found over the years to be one of the most powerful in its capability to reconstruct, with a minimum of errors, the velocity profile of handwritten strokes [25],[26],[41],[42]. This model is the kernel of the Kinematic Theory of Rapid Human Movements, initially proposed in the context of handwriting [25], [41] and later extended to process other bio-signals [2],[40]. This Theory describes the velocity profile of an end-effector by a Delta-Lognormal equation:

$$v(t) = D_1\Lambda(t; t_0, \mu_1, \sigma_1^2) - D_2\Lambda(t; t_0, \mu_2, \sigma_2^2) \quad (1)$$

where,

$$\Lambda(t; t_0, \mu, \sigma^2) = \begin{cases} \frac{1}{\sigma\sqrt{2\pi}(t-t_0)} \exp\left\{-\frac{1}{2\sigma^2}[\ln(t-t_0)-\mu]^2\right\} & \text{for } t > t_0 \\ 0 & \text{elsewhere} \end{cases} \quad (2)$$

and,

D_1, D_2 : the amplitudes of the input commands. Their effects correspond to the distances covered by the individual agonist (1) and antagonist (2) components.

t_0 : the time occurrence of the input commands, a time-shift parameter.

μ_1, μ_2 : the logtime delays, the time delays of the neuromuscular systems expressed on a logarithmic time scale. Explicitly, e^μ represents the median of a lognormal profile.

σ_1, σ_2 : the logresponse times, the response times of the neuromuscular systems expressed on a logarithmic time scale.

According to this representation, a rapid movement, produced by an end-effector, is the result of a synergy made up of an agonist and an antagonist neuromuscular systems. Each neuromuscular system is modeled by the convolution product of an infinite number of coupled subsystems and its corresponding impulse response converges toward a lognormal function. These impulse responses, once convolved with the input commands, represent respectively the agonist and the antagonist components of the velocity profile, which can be described synthetically by the seven parameters $(t_0, D_1, \mu_1, \sigma_1, D_2, \mu_2, \sigma_2)$ of the Delta-Lognormal pattern.

3 OUTLINES OF THE DELTA-LOGNORMAL EXTRACTOR

The functioning of the Delta-Lognormal extractor is schematised in Figure 1. Given a typical velocity profile $v(t)$, the algorithm first estimates the agonist lognormal parameters by considering $v(t)$ as a single lognormal profile. Then, the antagonist lognormal profile is deduct by subtracting the agonist lognormal profile from the velocity. The second step consists in the estimation of the antagonist lognormal parameters. Then, the estimated values of the seven parameters serve as a starting solution for an optimizing algorithm. Indeed, these initial estimated values may represent only a coarse solution depending on the experimental conditions under which handwriting data was collected. Starting from these coarse solutions, the extractor seeks for optimized values using a mean square nonlinear regression technique that minimizes the distance between experimental data and the predicted Delta-Lognormal model [43].

At the end of the process, one can obtain both the optimal values of the seven parameters and the mean square reconstruction error (MSE) between the original and the reconstructed velocity profiles.

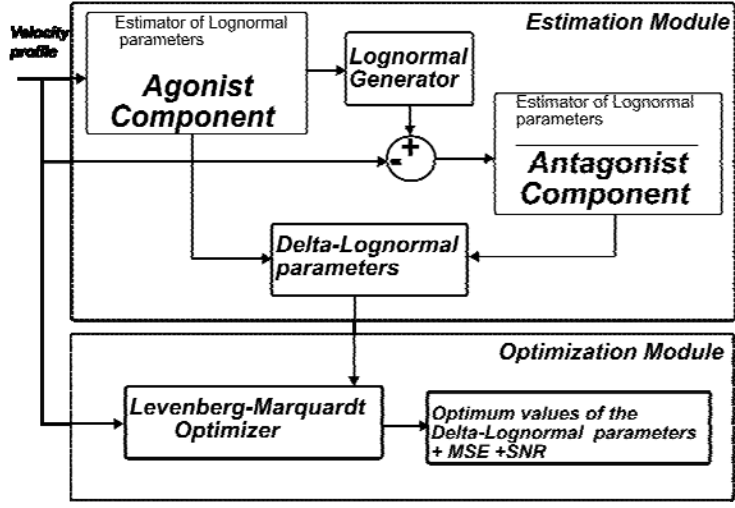


Fig 1: General architecture of the Delta-Lognormal extraction system

4. THE XZERO ALGORITHM

The previous architecture has been exploited by other algorithms in the past [31],[32] and it has been shown that its critical path was the initial estimation process: the better the starting solutions, the better the optimization results. Our new algorithm proposes an original solution to this estimation process; it exploits the analytical relationships that exist between three specific time-indexes of a lognormal profile $\Lambda(t)$ (a maximum and two inflexion points) and its four parameters. As illustrated in Figure 2, the time occurrence of the maximum corresponds to the solution of $d\Lambda(t)/dt = 0$ and the time occurrences of the inflexion points correspond respectively to the solutions of $d^2\Lambda(t)/dt^2 = 0$. For this reason, the new algorithm has been named XZERO, referring to these zero crossings.

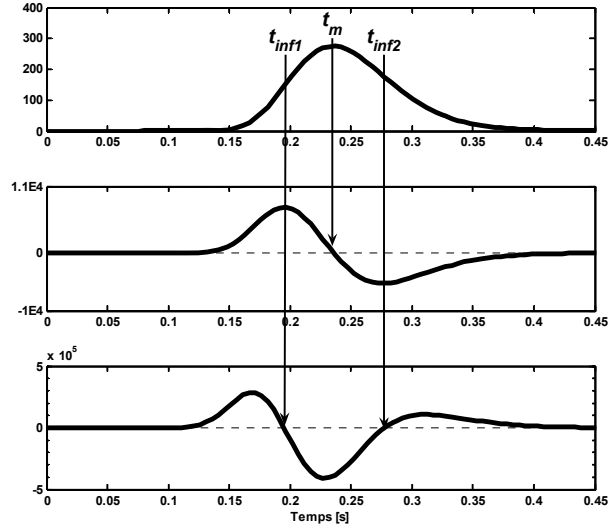


Fig 2. Illustration of a lognormal function and its first and second time-derivatives to highlight the time-indexes of the maximum and the inflexion points.

4.1. Estimation of lognormal parameters

The estimation of single lognormal parameters consists in linking the experimental values of these zero crossings to their corresponding analytical expressions.

Let consider $v(t; t_0, \mu, \sigma^2)$ be a lognormal function weighted by D and shifted by t_0 :

$$v(t; t_0, \mu, \sigma^2) = D\Lambda(t; t_0, \mu, \sigma^2) = \begin{cases} \frac{D}{\sigma(t-t_0)\sqrt{2\pi}} e^{-\frac{[\ln(t-t_0)-\mu]^2}{2\sigma^2}}, & t > t_0 \\ 0 & \text{elsewhere} \end{cases} \quad (3)$$

$$v(t; t_0, \mu, \sigma^2) = v(t, k) = \frac{D}{\sigma(t-t_0)\sqrt{2\pi}} e^{-\frac{k^2}{2}} \quad (4)$$

where $k = \frac{\ln(t-t_0)-\mu}{\sigma} \rightarrow \frac{dk}{dt} = \frac{1}{\sigma(t-t_0)}$

The first lognormal derivative is given by:

$$\frac{dv(t;k)}{dt} = \dot{v}(t;k) = \frac{d}{dt} \left[\frac{D}{\sigma(t-t_0)\sqrt{2\pi}} e^{-\frac{k^2}{2}} \right] = -\frac{v(t;k)}{\sigma(t-t_0)} (\sigma+k) \quad (5)$$

where \dot{v} and \ddot{v} are respectively the first and the second time-derivative of a function $v(t)$. The non-trivial zeros of this function occur when $\sigma+k=0$ v.g.:

$$\sigma+k=0 \rightarrow k = \frac{\ln(t-t_0) - \mu}{\sigma} = -\sigma \rightarrow t_m = t_0 + e^{\mu-\sigma^2}$$

The time occurrence of the maximum that corresponds to this zero crossing is given by:

$$t_m = t_0 + e^{\mu-\sigma^2} \quad (6)$$

Similarly, the second time-derivative of the shifted and weighted lognormal function is:

$$\begin{aligned} \frac{d^2}{dt^2}(v(t;k)) &= \ddot{v}(t;k) = \frac{d}{dt} \left(-v(t;k) \frac{\sigma+k}{\sigma(t-t_0)} \right) \\ &= \frac{v(t;k)}{\sigma^2(t-t_0)^2} (k^2 + 3k\sigma + 2\sigma^2 - 1) \end{aligned} \quad (7)$$

The zeros of this function are calculated by solving the following equation:

$$k^2 + 3\sigma k + 2\sigma^2 - 1 = 0 \quad (8)$$

Let $k_{1,2} = \frac{-3\sigma \pm \sqrt{\sigma^2 + 4}}{2}$ be the two solutions

Then, the roots are given by:

$$t_{\text{inf}1} = t_0 + \exp\left\{\mu - \sigma\left(\frac{3\sigma + \sqrt{\sigma^2 + 4}}{2}\right)\right\} = t_0 + \alpha_1 e^{\mu - \sigma^2} \quad (9.a)$$

$$t_{\text{inf}2} = t_0 + \exp\left\{\mu - \sigma\left(\frac{3\sigma - \sqrt{\sigma^2 + 4}}{2}\right)\right\} = t_0 + \alpha_2 e^{\mu - \sigma^2} \quad (9.b)$$

with

$$a_1 = \sigma\left\{\frac{\sigma + \sqrt{\sigma^2 + 4}}{2}\right\} > 0 \rightarrow \alpha_1 = e^{-a_1} < 1 \quad (10.a)$$

$$a_2 = \sigma\left\{\frac{\sigma - \sqrt{\sigma^2 + 4}}{2}\right\} < 0 \rightarrow \alpha_2 = e^{-a_2} > 1 \quad (10.b)$$

and

$$t_{\text{inf}1} < t_m < t_{\text{inf}2} \quad (11)$$

In practice, these three time indexes are calculated from sampled velocity profiles by considering the time occurrences of the maximum velocity to estimate t_m and the time occurrences of the maximum and the minimum of the acceleration to estimate $t_{\text{inf}1}$ and $t_{\text{inf}2}$ respectively.

Thus, by using (6), (9.a) and (9.b) one can express t_0, D, μ and σ as a function of $t_m, t_{\text{inf}1}$ and $t_{\text{inf}2}$.

4.1.1 Estimation of σ

The parameter σ is estimated by solving a non-linear equation. Indeed, let consider the interval I , which covers 99.97% of the surface under a lognormal curve:

$$I = [e^{\mu-3\sigma}, e^{\mu+3\sigma}] = [t_{\min}, t_{\max}] \quad (12)$$

where t_{\min} and t_{\max} are the extreme bounds of the interval, as estimated from the lognormal profile using empirical thresholds (v.g. the times when the velocity reaches 1% of its maximum). Then:

$$e^{\mu+3\sigma} - e^{\mu-3\sigma} = e^{\mu} (e^{3\sigma} - e^{-3\sigma}) \square t_{\max} - t_{\min} \quad (13)$$

$$e^{\mu} \square \frac{t_{\max} - t_{\min}}{2 \sinh(3\sigma)} \quad (14)$$

$$t_m - t_{\min} \square e^{\mu} [e^{-\sigma^2} - e^{-3\sigma}] \quad (15)$$

and finally, σ is evaluated by solving the following nonlinear relationship:

$$F(\sigma) = \frac{t_{\max} - t_{\min}}{2 \sinh(3\sigma)} [e^{-\sigma^2} - e^{-3\sigma}] - (t_m - t_{\min}) = 0 \quad (16)$$

4.1.2. Estimation of the other parameters

Using the estimated value $\hat{\sigma}$ of σ , the estimated value $\hat{\mu}$ of μ can be computed by:

$$t_{\text{inf}2} - t_{\text{inf}1} = e^{\hat{\mu} - \hat{\sigma}^2} (e^{-\hat{\alpha}_2} - e^{-\hat{\alpha}_1}) = (\hat{\alpha}_2 - \hat{\alpha}_1) e^{\hat{\mu} - \hat{\sigma}^2} \quad (17)$$

$$\hat{\mu} = \hat{\sigma}^2 + \ln \left(\frac{t_{\text{inf}2} - t_{\text{inf}1}}{\hat{\alpha}_2 - \hat{\alpha}_1} \right) \quad (18)$$

with $\hat{\alpha}_1$ et $\hat{\alpha}_2$ the estimated values of α_1 and α_2 . Then one can estimate t_0 :

$$\hat{t}_0 = t_m - e^{\hat{\mu} - \hat{\sigma}^2} \quad (19)$$

and D, using:

$$v(t_m) = v_m = \frac{D}{\hat{\sigma}(t_m - \hat{t}_0)\sqrt{2\pi}} e^{-\frac{1}{2\hat{\sigma}^2}(\ln(t_m - \hat{t}_0) - \hat{\mu})^2} \quad (20)$$

$$v_m = \frac{D}{\hat{\sigma}\sqrt{2\pi}e^{\hat{\mu} - \hat{\sigma}^2}} e^{-\frac{1}{2\hat{\sigma}^2}(\hat{\mu} - \hat{\sigma}^2 - \hat{\mu})^2} = \frac{D}{\hat{\sigma}\sqrt{2\pi}} e^{-\hat{\mu} + \frac{\hat{\sigma}^2}{2}} \quad (21)$$

$$\hat{D} = v_m \hat{\sigma} \sqrt{2\pi} e^{\hat{\mu} - \frac{\hat{\sigma}^2}{2}} \quad (22)$$

where v_m is the maximum velocity.

4.2. Estimation of the Delta-Lognormal parameters

The estimation of the agonist lognormal parameters is performed by exploiting directly the above method since a Delta-Lognormal profile is given by:

$$v(t) = v_1(t) - v_2(t) \quad (23)$$

where $v_1(t)$ and $v_2(t)$ are respectively the agonist and the antagonist components. Using (16) to (22), the agonist parameters are estimated by considering the main peak of the velocity profile as a single lognormal function ($v(t) \approx v_1(t)$, $t_{\text{inf}1} < t < t_{\text{inf}2}$).

The antagonist parameters are then evaluated after subtracting the agonist component $v_1(t)$. From the total velocity profile $v(t)$. The time indexes of the resulting lognormal function $v_2(t)$ are given by:

$$t_{m2} = t_0 + e^{\mu_2 - \sigma_2^2} \quad (24)$$

$$t_{\text{inf}12} = t_0 + e^{\mu_2 - \sigma_2^2} e^{-a_1} \quad (25)$$

$$t_{\text{inf}22} = t_0 + e^{\mu_2 - \sigma_2^2} e^{-a_2} \quad (26)$$

The following expressions are then used to estimate σ_2 :

$$\frac{t_{\text{inf}22} - t_0}{t_{\text{inf}12} - t_0} = \frac{e^{\mu_2 - \sigma_2^2} e^{-a_2}}{e^{\mu_2 - \sigma_2^2} e^{-a_1}} = e^{a_1 - a_2} \quad (27)$$

Considering $B = a_1 - a_2 = \ln\left(\frac{t_{\text{inf}22} - t_0}{t_{\text{inf}12} - t_0}\right)$, a positive constant:

$$t_{\text{inf}12} < t_{\text{inf}22} \rightarrow 1 < \frac{t_{\text{inf}22} - t_0}{t_{\text{inf}12} - t_0} \rightarrow 0 < B = \ln\left(\frac{t_{\text{inf}22} - t_0}{t_{\text{inf}12} - t_0}\right) \quad (28)$$

$$a_1 - a_2 - B = \frac{\sigma_2}{2}(\sigma_2 + \sqrt{\sigma_2^2 + 4}) - \frac{\sigma_2}{2}(\sigma_2 - \sqrt{\sigma_2^2 + 4}) - B = 0 \quad (29)$$

then

$$\sigma_2^2(\sigma_2^2 + 4) = B^2 \quad (30)$$

Using $l = \sigma_2^2$, equation (30) becomes a second order polynomial:

$$l^2 + 4l - B^2 = 0 \quad (31)$$

The parameter σ_2 is calculated from the positive solution of (31):

$$\hat{\sigma}_2 = \sqrt{\sqrt{B^2 + 4} - 2} \quad (32)$$

The estimated value $\hat{\mu}_2$ of the parameter μ_2 is computed by the following expression:

$$\hat{\mu}_2 = \hat{\sigma}_2^2 + \ln \left[\frac{t_{\text{inf}22} - t_{\text{inf}12}}{A} \right] \quad (33)$$

with

$$A = e^{-\hat{a}_{22}} - e^{-\hat{a}_{12}} \quad (34)$$

and finally, the estimated value \hat{D}_2 of D_2 is given by:

$$\hat{D}_2 = v_{2\text{max}} \hat{\sigma}_2 \sqrt{2\pi} e^{\hat{\mu}_2 - 0.5\hat{\sigma}_2^2} \quad (35)$$

where $v_{2\text{max}}$ is the maximum value of $v_2(t)$.

5. TESTING UNDER IDEAL CONDITIONS

After implementing XZERO on a software benchmark, a testing phase under ideal conditions has been performed. It consisted in building an ideal database of Delta-Lognormal functions, and comparing the performances of our new algorithm with two previously developed deterministic algorithms: INFLEX [31] and INITRI [32]. INFLEX uses a graphical method for the initial estimation, based on the characteristics of the tangents of the inflexion points of the main velocity peak, while INITRI uses analytical relationships

between the parameters and the time occurrence of the maximum velocity and two other arbitrary points located in the rising phase of the velocity curve.

5.1. Construction of the database

Theoretically, one can generate an infinite number of velocity profiles from the superposition of two agonist and antagonist lognormal components. The construction of our database aimed at grouping this large variety into a few classes. To reach this goal, two main features were considered to classify the ideal profiles into seven classes (i) the number of zero crossings appearing in the velocity profile, and (ii) the position of the antagonist component with respect to the agonist one [40]. Figure 3 depicts typical examples for each class C_{uw} , where the subscript **u** indicates where the dominance of the antagonist component occurs with respect to the antagonist one (**b** : before, **a**: after or **s**: simultaneous) and the subscript **w** represents the number of zero crossings **0**, **1** or **2**. The label **i** (imaginary) is used when there is no real roots to the zero crossing equation [32],[41]. As one can see in these plots, the different timings of the antagonist versus the agonist curves generate a large variety of primitive patterns.

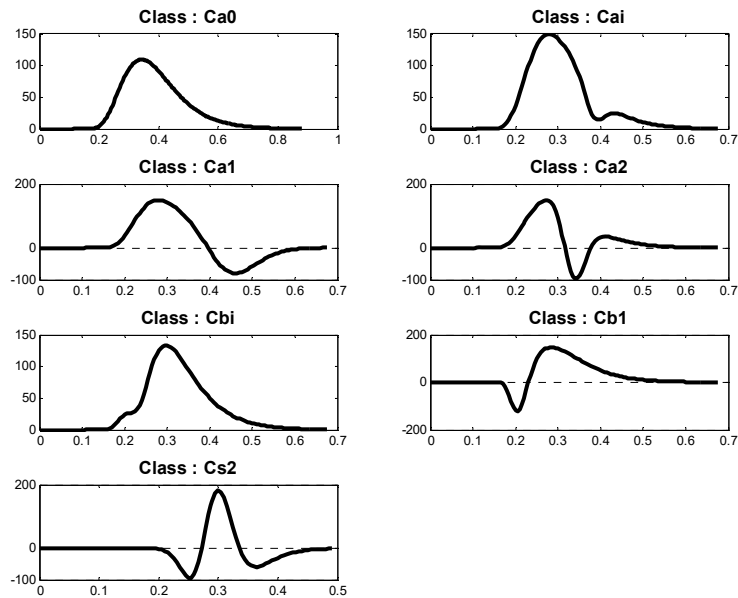


Fig 3. The seven classes of Delta-Lognormal velocity profiles as generated by a synergy of an artificial agonist and antagonist neuromuscular systems.

This wide variability is obtained by randomly selecting the Delta-Lognormal parameter values within specific intervals, these intervals being fixed according to typical features of rapid movements. In this data base, we assumed that the movement time was typically between 100 ms and 500 ms, and the minimum time occurrence of the maximum about 100 ms, as measured from t_0 . The lower bound of this latter parameter was fixed considering the fact that a human being does not respond without anticipation to a stimulus faster than 50 ms. The upper bound was arbitrary fixed at one second. The parameters D_1 and D_2 were empirically deduct by taking into account both the dimension of the digitizer used to acquire real data (31cmx23 cm) and the assumption that the distance covered by the antagonist movement was smaller than the one covered by the agonist.

The corresponding ratio was fixed to $D_{2\max} \approx 0.1D_{1\max}$ to emulate worst-case testing conditions [34] (see Table 1).

TABLE 1. VARIATION RANGES OF THE DELTA-LOGNORMAL PARAMETERS [34]

<i>Parameters</i>	<i>Min</i>	<i>Max</i>
t_0 (s)	0.05	1.0
	5	70
D_2 (cm)	0.5	7
μ_1, μ_2	-2.2	-1.6
σ_1, σ_2	0.1	0.45

5.2. Performance evaluation

To test our algorithm, each ideal Delta-Lognormal curve was sampled at 200Hz to simulate the data collected from a digitizer. The seven parameter values extracted by the XZERO, INFLEX and INITRI algorithms were compared with the original ones (Truth Table). The results are summarized in Table 2 [32],[40]. In this test, the extracted parameters were considered as matching the original ones if the signal to noise ration (SNR) between the original and the reconstructed curve was greater than 100 dB (equivalent to a Mean Square Error (MSE) of less than $10^{-9} \text{ cm}^2 \cdot \text{s}^{-2}$).

As one can see from Table 2, for the C_a classes (antagonist dominance after the agonist peak activity), XZERO performs better than INFLEX and INITRI, both of which have also serious problems with the C_b classes, where the antagonist activity is dominant before the agonist activity. If we remove the results from these two classes, we can see, in the penultimate column, that there are 6% and 12% differences between XZERO and the other two algorithms respectively. These differences grow up to 30% and 32% respectively (last column) when all the specimens are taken into account.

However, a vertical comparison of the results in Table 2 emphasizes the complementarities of the three algorithms. This is mainly due to the fact that INFLEX encounters some difficulties when the main peak of the velocity profile is almost symmetric, while INITRI has some troubles with profiles that are deeply asymmetric. Moreover, XZERO has a stable performance with a minimum of 92 % of perfect reconstruction for ideal Delta-Lognormal curves.

In an attempt to improve these capabilities, we have thus designed a combined system, called INFLEX+INITRI+XZERO or (IIX) which integrates the three algorithms in parallel. For each test curve, the solution, chosen among the solutions given by the three algorithms, corresponds to the one that leads to a minimum mean square error. As one can see from Table 2, the IIX system is better than XZERO, INFLEX and INITRI, considered individually. The IIX system can recover 100% of the original parameters for the C_a classes and 99.3% when all the database profiles are analyzed. Considering the improvements resulting from the parallel use of the three algorithms, we have adopted this architecture as an upgrade of our extractor system and used it in the next study.

TABLE 2: RESULTS OF THE TESTS UNDER IDEAL TESTING CONDITIONS

(PERFORMANCE CRITERION: $SNR \geq 100$ dB)

<i>Performances</i> <i>Class</i>	C_{bi}	C_{bt}	C_{a0}	C_{ai}	C_{at}	C_{a2}	C_{s2}	<i>Downstream</i>	<i>All</i>
	[%]	[%]	[%]	[%]	[%]	[%]	[%]	<i>only</i>	
<i>Method</i> INFLEX	0	9	90.1	94.6	91.9	94.6	92.8	92.8	66.41
INITRI	3	37.1	74.7	92.1	80.7	100	65.8	86.87	64.38
XZERO	98.1	97.9	95.2	100	96.6	100	92	98.2	97.1
IIX	98.1	98.5	99.7	100	99.5	100	99.6	100	99.3

6. PERFORMANCES UNDER NOISY CONDITIONS

In real situations, the strokes acquired from a digitizer usually contain noise and distortion. Moreover, there is no prior information about the original values of the seven parameters. Therefore, the extracted data are corrupted by error sources and the resulting extraction errors must be circumscribed to quantify the accuracy of the extractor under noise constraints. To do so, another database has been constructed by adding to the ideal data sets an artificial noise with zero mean and various levels of signal to ratio, using a Gaussian random noise generator [32],[40].

Figure 4 shows a pair of such noisy profiles (with SNR = 20 dB), as constructed from two of the profiles presented in Figure 3.

A first evaluation of performance based on the percentages of successful extractions, using corrupted profiles with SNR of 20 dB has been run. In this experiment, a solution was accepted if the signal to noise ratio (SNR) of the reconstructed profile was greater than an arbitrary threshold of 10 dB. As one can see in Table 3, XZERO performed better than INFLEX and INITRI under these noisy conditions, and the combined system IIX converged in more than 98% of the cases.

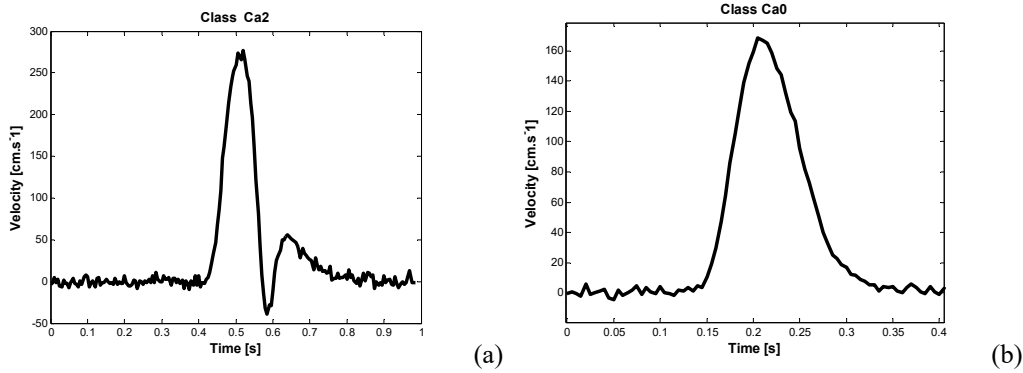


Fig 4. Two noisy Delta-Lognormal profiles that correspond to two of the ideal profiles depicted in Figure 3 (classes Ca2 and Ca0, respectively), upon which a 20dB noise has been superimposed.

Since we knew the original parameter values of each noisy curve in this simulation, we could evaluate the performance of the extractor according to its capability to recover, under various SNR, the real parameter values within specific confidence intervals.

For example, Figure 5 depicts the extracted values of the parameter σ_1 vs. the original ones, for SNR equal to 20, 30, 40 and 50 dB respectively. Each plot represents the best extraction result as obtained by the IIX system. For ideal curves, all dots in a plot would be located on the 45° oblique line and, in noisy conditions, the extraction errors result in a dispersion of the values around this oblique line. As can be observed from these plots, there is a relationship between the dispersion error and the SNR. Indeed, Figure 6a depicts the extraction error of the parameter σ_1 for a SNR equal to 20 dB; these fluctuations look like a random signal. Its histogram (Figure 6b) shows that the error roughly follows a Gaussian process. According to a Kolmogorov-Smirnov test, this histogram can be considered as a normal distribution ($h=0$, $p=0.03$), and we can thus evaluate, for each parameter, the dispersion of the corresponding extraction error through its confidence interval. This result suggests that a part of the synthetic Gaussian noise added to the ideal velocity profile is transformed into an extraction error that keeps the same distribution. In

other words, the IIX extractor can be considered as a system that does not generate any additional distortion or noise to the Delta-Lognormal parameters but that translates the noise existing in the original data into extraction errors. In these conditions, confidence intervals can be estimated for the optimal extracted values of the seven parameters.

TABLE 3 RESULTS OF THE TESTS UNDER NOISY CONDITIONS IN THE CASE OF SNR = 20 dB

(CONVERGENCE CRITERION: $SNR \geq 10$ dB)

Algorithms	<i>NOISY DATA</i>				
	% of convergence	MSE _{mean}	MSE _{std}	SNR _{mean}	SNR _{std}
	(from 7000 curves)	[cm ² /s ²]	[cm ² /s ²]	[dB]	[dB]
INFLEX	63.24	32.90	62.44	21.76	2.13
INITRI	82.90	31.98	60.91	21.62	2.28
XZERO	95.69	30.28	59.32	21.32	2.05
IIX	98.81	28.62	60.20	21.63	2.26

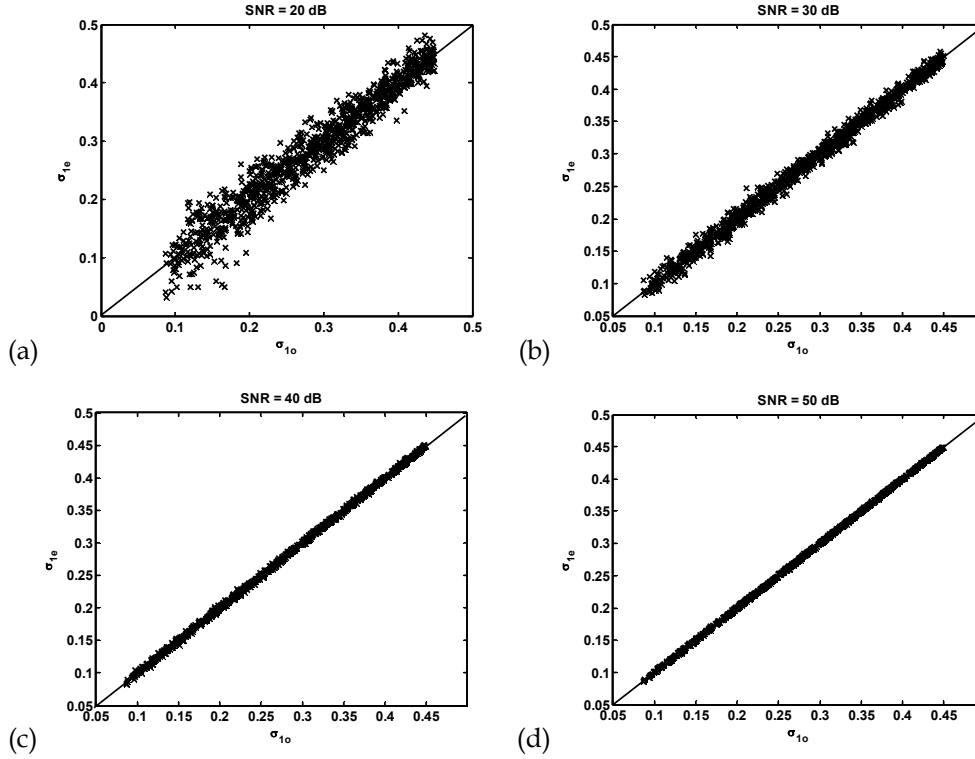


Fig 5. A typical result of the extracted error dispersion according to SNR values. Representation of the extracted values versus the original ones for the parameter σ_1 at different noise levels.

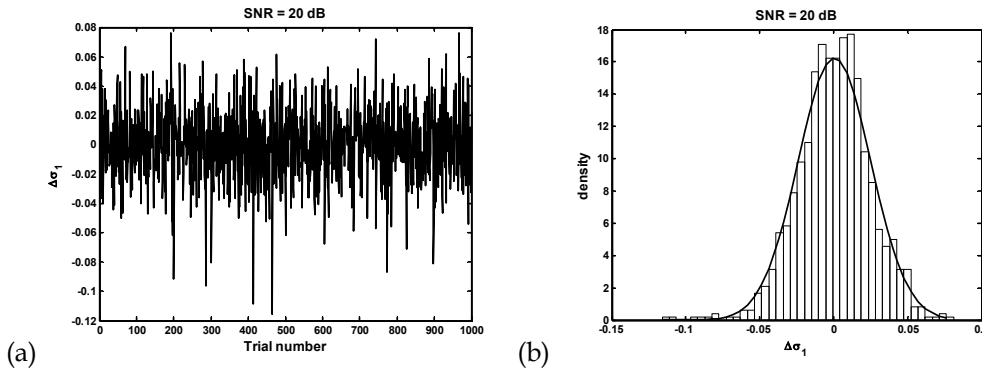


Fig 6. a) Typical result of the extraction error profile of the parameter σ_1 as obtained for SNR =20 dB and for the C_{σ_0} class b) Its corresponding histogram assimilated to a Gaussian density, the continuous curve represents a Gaussian density as calculated by a Kolmogorov-Smirnov test with $h=0$ and $p=0.03$.

6.1. Evaluation of the extraction accuracy

The second performance evaluation relied on the circumscription and the quantification of the extractor accuracy by constructing these confidence intervals (CI) for each parameter. This has been computed using the optimal parameter values, the MSE and the SNR.

To do so, the extracted value of a parameter was considered as the center of a confidence interval with extremities calculated from the standard deviation STD of the corresponding extraction error. For example, the CI of the parameter σ_1 was computed by:

$$CI_{\sigma_1} = [\sigma_1 - k * STD_{\sigma_1}, \sigma_1 + k * STD_{\sigma_1}] \quad (36)$$

where σ_1 is the extracted value, STD_{σ_1} the standard deviation of the extraction error and k the dispersion range ($k=1, 2$ or 3). Let us recall that for $k=2$, the original value is inside the CI with a confidence level of 95%.

Since the dispersion STD decreases when the SNR increases (see Figure 5), one can construct empirical relationships between these quantities and build the confidence intervals CI from the SNR values.

These empirical relationships were calculated as follows: for each Delta-Lognormal parameter, a dispersion parameter STD_p of the extraction error was calculated (assuming that the mean value of the error was nearly zero) by considering the 7000 curves of the seven classes, for a given SNR value. The STD_p versus SNR curve was then plotted as , for examples, in Figures 7. An exponential relationship emerges from these plots, which can be expressed as:

$$STD_p = \alpha e^{-\beta SNR} \quad (37)$$

where STD_p is the standard deviation of the extraction error for a given parameter p , and α and β are the regression coefficients, as summarized in Table 4 for the seven parameters. According to the definition of the SNR ($SNR = 10 \log_{10} [P_s/P_n]$) where P_s is the

power of the signal and $P_n = STD_n^2$ is the power of the Gaussian noise), equation (37) can be rewritten as follows:

$$STD_p = \frac{\alpha}{P_s} STD_n \quad (38)$$

TABLE 4: EXPONENTIAL REGRESSION RESULTS WITH THE CORRESPONDING CORRELATION COEFFICIENTS r^2 .

<i>Parameters</i>	α	β	r^2
t_0	0.13	0.129	0.97
D_1	6.8	0.117	0.99
μ_1	1.37	0.103	0.98
σ_1	0.3	0.117	0.99
D_2	7.63	0.113	0.99
μ_2	2.45	0.104	0.97
σ_2	0.31	0.113	0.99

Equation (38) clearly reflects the fact that the power of the extraction error (its standard deviation) corresponds to a proportion of the noise added to the velocity profiles. As previously anticipated, this also suggests that the IIX extractor does not add any supplementary noise but “transforms” the existing fluctuations into extraction errors with different proportions.

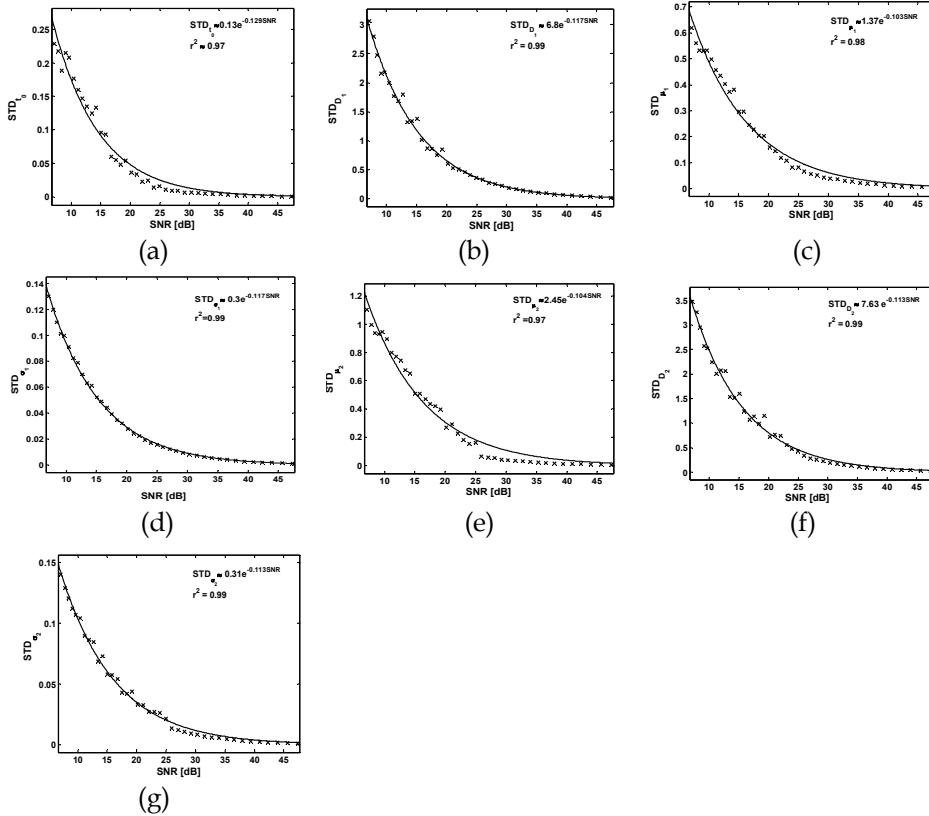


Fig 7. Typical results depicting exponential regressions between the standard deviation of the extraction errors and the SNR of the noisy Delta-Lognormal profiles

This characterization process permits the quantification of the extractor accuracy and the determination of confidence intervals for each extracted parameter value.

7. TESTING WITH REAL DATA

To evaluate the performance of the IIX extraction system in real applications, we have conducted a third experiment using real handwritten strokes sampled at 200 Hz with a Wacom Intuos II digitizer. Figure 8a depicts a typical x-y trajectory of a stroke produced by a human subject. The corresponding velocity profile, as illustrated in Figure 8b, was computed using numerical filters (a Chebychev II low-pass filter with order $n=10$, cutoff frequency $F_c=16$ Hz, sampling frequency $F_s=200$ Hz, and Attenuation $Att=-81$ dB, and a FIR derivative filter with $n=10$, $F_c=50$ Hz and $F_s=200$ Hz) applied to the two posi-

tion components $x(t)$ and $y(t)$ for each stroke. Representative results of the analysis-by-synthesis process are presented in Figures 9a-d. For each trial, the velocity profile, as reconstructed from the seven extracted parameters, is very close to the original profile with SNR greater than 20 dB. Details of the corresponding parameters with their confidence intervals are summarized in Table 5.

As one can deduct from this Table, the agonist parameters were extracted with more accuracy (extraction uncertainty less than 9 %) than the antagonist ones. This was probably caused by both the architecture of the extractor and the fact that the antagonist parameter values were small. Indeed, since the antagonist component is isolated after subtracting the estimated agonist component, this creates more distortions in the antagonist profile and leads to a poorer estimation of its parameters.

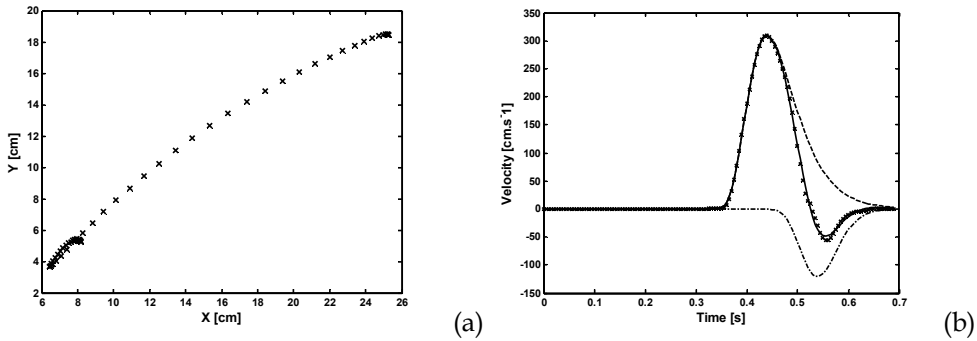


Fig 8. Typical example of real data. a) stroke trajectory; b) velocity profile (cross: original profile; solid line: reconstructed profile, dashed lines: agonist and antagonist components respectively).

Moreover, since the magnitude of D_2 is generally smaller than D_1 and becomes often comparable to the magnitude of the noise, it is difficult to get an acceptable precision in some cases. For example, in the velocity profiles depicted in Figure 9-a, the uncertainty grows up to 32% when D_2 is small even if the SNR is about 31 dB. However, as depicted in Figures 9-b and 9-d, when the antagonist component is more significant, the corresponding uncertainty of its parameters decreases, to less than 20% in these specific results.

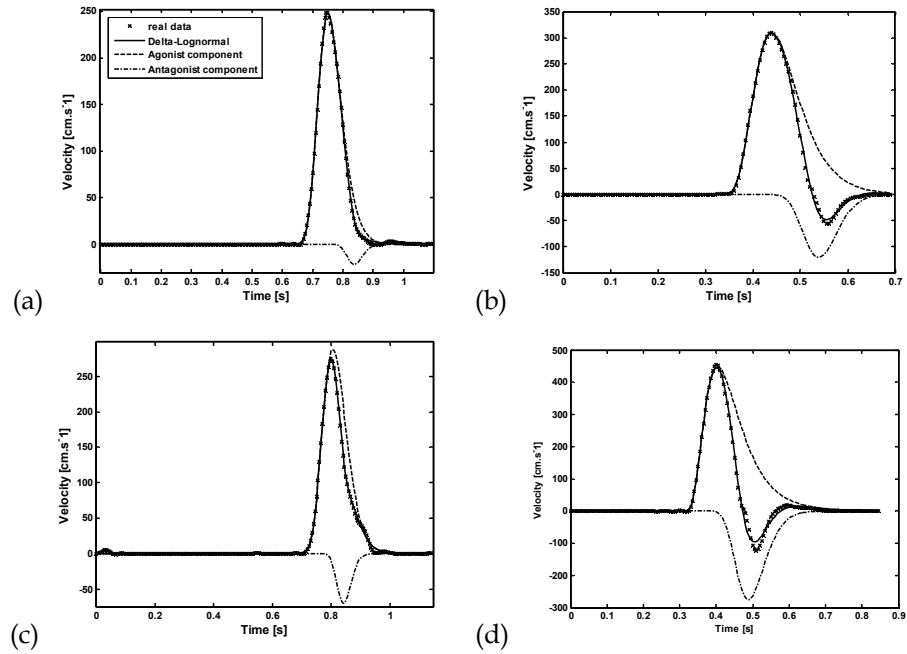


Figure 9: typical extraction results from different velocity patterns. The corresponding parameter values are summarized in Table 5.

TABLE 5. SUMMARY OF EXTRACTED PARAMETER VALUES WITH CONFIDENCE INTERVALS EXPRESSED IN TERMS OF PERCENTAGES.

<i>Parameter</i>	t_0	D_1	μ_1	σ_1	D_2	μ_2	σ_2	MSE	SNR
<i>Trial #</i>	(s)	(cm)			(cm)			($cm^2.s^2$)	(dB)
a	0.567	24.733	+/- -1.651	0.212	1.32	-1.3	0.091	4.86	31.79
	+/- 1.3%	1.56%	+/-4.72%	+/-8.04%	+/- 32.86%	+/-10.71%	+/-19.37%		
b	0.302	38.214	+/- -1.867	0.338	10.876	-1.418	0.15	20.66	29.45
	+/- 3.8%	1.31%	+/-5.42%	+/-6.56%	+/- 5.18%	+/-18.76%	+/- 15.26%		
c	0.603	29.762	+/- -1.556	0.199	4.204	-1.421	0.099	4.15	34.14
	+/- 0.94%	0.99%	+/-3.85%	+/-6.58%	+/-7.93%	+/-7.53%	+/- 13.62%		
d	0.3	61.22	-2.046	0.471	27.703	-1.626	0.209	92.58	24.15
	+/- 5.79%	+/- 1.48%	+/-8.95%	+/-8.52%	+/- 3.68%	+/-20.15%	+/- 19.84%		

8. CONCLUSION

In this paper, we have focused on the analysis-by-synthesis of individual strokes, i.e. the study of motor control primitives. Using the Kinematic Theory, which completely describes the velocity profile of rapid movement with seven Delta-Lognormal parameters, we have developed an efficient parameter extractor system that relies on a new algorithm (XZERO). This algorithm exploits the properties of the first and the second time-derivatives of a lognormal function. We have highlighted the performance improvements that are observed by this new estimation method in comparison with two existing ones (INFLEX and INITRI). For ideal curves, XZERO finds the true values of Delta-Lognormal parameters in 97% of the cases, for a database of 7000 curves representing a huge variety of patterns. Moreover, the complementarities that exist between the three algorithms (INFLEX, INITRI and XZERO) have led us to combine them in a new architecture, the IIX system, to improve the global performances.

We have also circumscribed and quantified the confidence intervals of the extracted values, exploiting the empirical exponential regressions that link the standard deviation (STD) of the extraction error with the SNR. Thus, the optimal values of the parameters used to reconstruct the velocity profiles of rapid movements by a Delta-Lognormal equation are, for the first time, accompanied with precision estimates, which quantify their relative validity.

One useful application of this new information is for the calibration of Delta-Lognormal measurement systems. Although more works will be necessary to apply this technology to the study of complex movements like handwriting, the present tool already offers the possibility of analyzing the behavior of neuromuscular and motor control sys-

tems under various experimental and psychophysical conditions, through the variations in the parameter values.

With this robust extractor, the Kinematic Theory will become more attractive for the study of movement primitives. Current experiments are going on in our laboratory, where, for example, our algorithms are applied to analyze the intrinsic properties of strokes produced by different group of participants (young and aged subjects, male and female, etc) [6,44], and to provide a better understanding of these primitives and their use as building blocks for the automatic processing of handwriting in various fields of computer science [2],[3]. In its present form, the IIX system is not limited to human movement applications. It could be employed to analyze any lognormal processes. Its generalization and adaptation to the study of more complex patterns is under way.

ACKNOWLEDGEMENTS

This research work was supported by NSERC grant RGPIN-915 to Réjean Plamondon.

REFERENCES

- [1] M. Djioua and R. Plamondon, "Analysis and Synthesis of Handwriting Variability using the Sigma-Lognormal Model," *Proceeding of the 13th Conference of the International Graphonomics Society (IGS2007)*, vol 13, pp. 19-22, 2007.
- [2] R. Plamondon and M. Djioua, "A multi-level representation paradigm for handwriting stroke generation," *Human Movement Science*, vol. 25, pp. 586-607, 2006.
- [3] R. Plamondon, and M. Djioua, "Handwriting Stroke Trajectory Variability in the context of the Kinematic Theory," *Proceeding of the 12th Conference of the International Graphonomics Society (IGS2005)*, vol 12, pp. 250–254, 2005.

- [4] R. Plamondon, and S. Srihari, "On-line and off-line handwriting recognition: A comprehensive survey," *20th Anniversary Special Issue. IEEE Trans. On Pattern Analysis and Machine Intelligence*, vol. 22, pp. 63–84, 2000.
- [5] R. Plamondon, D. Lopresti, L.R.B. Schomaker, and S. Srihari, "On-line handwriting recognition," In J. G. Webster (Ed.). *Wiley Encyclopedia of Electrical and Electronics Engineering*, vol. 15, pp. 123-146, 1999, NY: John Wiley & Sons, ISBN0-471-13946-7.
- [6] A. Woch, "Étude des primitives bidirectionnelles du mouvement dans le cadre de la théorie cinématique: confirmation expérimentale du modèle delta-lognormal," PhD dissertation, Dept. of Electrical, École Polytechnique de Montréal, 2006.
- [7] A. Woch and R. Plamondon, "The problem of Movement Primitives in the Context of the Kinematic Theory," *Proceeding of the 11th Conference of the International Graphonomics Society (IGS2003)*, Scottsdale, Arizona, USA, vol. 11, pp. 67-71, 2003.
- [8] A. Woch and R. Plamondon, "Using the Framework of the Kinematic Theory for the Definition of a Movement Primitive," *Motor Control*, vol. 8, pp. 547-557, 2004.
- [9] S. F. Giszter, F. A. Mussa-Ivaldi, and E. Bizzi, "Convergent Force Field Organized in the Frog's Spinal Cord," *Journal of Neuroscience*, vol. 13, pp. 467-491, 1993.
- [10] F. A. Mussa-Ivaldi, S. F. Giszter, and E. Bizzi, "Linear combinations of primitives in vertebrate motor control," *Proceedings of the National Academy of Sciences, USA*, vol. 91(16), pp. 7534-7538, 1994.
- [11] R. W. Paine and J. Tani, "Motor primitive and sequence self-organization in a hierarchical recurrent neural network," *Neural Network*, vol. 17, pp. 1291-1309, 2004.
- [12] K. A. Thoroughman and R. Shadmehr, "Learning of action through adaptive combination of motor primitives," *Nature*, vol. 407, pp. 742-747, 2000.

- [13] O. Hilton, "Scientific Examination of Questioned Documents," *In CRC series in forensic and police science*, 1993, CRC Press, Boca Raton, London, revised edition.
- [14] M.L. Simner and P.L. Girouard (Eds.), "Advance in forensic document examination [Special issue]," *Journal of Forensic Document Examination*, vol. 13, pp. 1–14, 2000.
- [15] M.L. Simner, C.G. Leedham, and A. J. W. M. Thomassen, (Eds.), "Handwriting and drawing research: Basic and applied issues," Amsterdam: IOS Press, 1996.
- [16] J. Wann, A.M. Wing, and N. Søvik, "Development of graphic skills: Research, perspectives and education implications. London: Academic Press, 1991.
- [17] A. Schröter, R. Mergl, K. Bürger, H. Hampel, H.-J Möller and U. Hegerl, "Kinematic analysis of handwriting movements in patients with Alzheimer's disease, mild cognitive impairment, depression and healthy subjects," *Dementia and Geriatric Cognitive Disorders*, vol. 15, pp. 132–142, 2003.
- [18] H. L. T. Teuling and G.E. Stelmach, "Control of stroke size, peak acceleration and stroke duration in Parkinsonian handwriting," *Human Movement Science*, vol. 10, pp. 315–333, 1991.
- [19] B. Rohrer, S. Fasoli, H.I. Krebs, R. Hughes, B. Volpe, and W.R. Frontera, "Movement smoothness changes during stroke recovery", *Journal of Neuroscience*, vol. 22, pp. 8297–8304, 2002.
- [20] V. Potkonjak, "Robotic handwriting", *International Journal of Humanoid Robotics*, vol. 2, pp.105–124, 2005.
- [21] F. Lacquaniti, C. Terzuolo, and P. Viviani, "The law relating the kinematic and figural aspects of drawing movements," *Acta Psychologica*, vol. 54, pp. 115-130, 1983.

- [22] P. Morasso, "Spatial control of arm movements," *Experimental Brain Research*, vol. 42, pp. 223-227, 1981.
- [23] J. Soechting and F. Lacquaniti, "Invariant characteristics of a pointing movement in man," *Journal of Neuroscience*, vol. 1, pp. 710-720, 1981.
- [24] P. Viviani and C. Terzuelo, "Space-time invariance in learned motor skills," *In: Stelmach GE, Requin J (eds) Tutoriels in motor behavior. North-Holland, Amsterdam*, pp 525-533, 1980.
- [25] R. Plamondon, "A kinematic theory of rapid human movements Part I. Movement representation and generation," *Biological Cybernetics*, vol. 72, pp. 295-307, 1995.
- [26] R. Plamondon and W. Guerfali, "The generation of handwriting with delta-lognormal synergies," *Biological Cybernetics*, vol. 78, pp. 119-132, 1998.
- [27] W. Guerfali, "Modèle Delta-lognormal vectoriel pour l'analyse du mouvement et la génération de l'écriture manuscrite," Ph.D. dissertation, Dept. of Electrical, École Polytechnique de Montréal, 1996.
- [28] F. Leclerc, "Modèle de génération de mouvements rapides en représentation de signatures manuscrites," Ph.D. dissertation, Dept. of Electrical, École Polytechnique de Montréal, 1996.
- [29] A. C. Cohen and B. J. Whitten, "Estimation in the Three-Parameter Lognormal Distribution," *Journal of the American Statistical Association*, vol. 75(370), pp. 399-404, 1980.
- [30] E. L. Crow and K. Shimizu (Eds.), "Lognormal distributions: theory and applications," vol. 88, Dekker, 1988.

- [31] W. Guerfali and R. Plamondon, "Signal processing for the Parameter Extraction of the Delta Lognormal Model," *Research in Computer and Robot Vision*, pp. 217-232, 1995.
- [32] R. Plamondon, X. Li, M.Djioua, "Extraction of delta-lognormal parameters from handwriting strokes," *Journal of Frontiers of Computer Science in China*, vol. 1(1), pp:106-113, 2007.
- [33] M. Djioua, R. Plamondon, A. Della Cioppa, A., Marcelli, "Delta-lognormal parameter estimation by non-linear regression and evolutionary algorithm: A comparative study," *Proceeding of the 12th Conference of the International Graphonomics Society (IGS2005)*, vol. 12, pp. 44-48, 2005.
- [34] M. Djioua, R. Plamondon, A. Della Cioppa, A., Marcelli, "Deterministic and evolutionary extraction of Delta-Lognormal parameters: performance comparison," *International Journal of Pattern Recognition and Artificial Intelligence*, vol. 21(1), pp. 21-41, 2007.
- [35] T. Varga, D. Kilchhofer, H. Bunke, "Template-based Synthetic Handwriting Generation for the Training of Recognition Systems," *Proceeding of the 12th Conference of the International Graphonomics Society (IGS2005)*, vol. 12, pp. 206-211, 2005.
- [36] R. Plamondon, A. M. Alimi, P. Yergeau, and F. Leclerc, "Modelling velocity profiles of rapid movements: a comparative study," *Biological cybernetics*, vol. 69(2), pp. 119-128, 1993.
- [37] A. Alimi, "Contribution au développement d'une théorie de génération de mouvements simples et rapides: application au manuscrit," Ph.D. dissertation, Dept. of Electrical, École Polytechnique de Montréal, 1995.

- [38] A. Alimi and R. Plamondon, "A comparative study of speed/accuracy tradeoff formulations: The case of spatially constrained movements where both distance and spatial precision are specified," in M. L. Simner, G. Thomassen, A.J.T.W.M., Eds. *Handwriting and drawing research: basic and applied issues*. IOS Press, Amsterdam, pp. 127-142, 1996.
- [39] C. Feng, A. Woch, and R. Plamondon, "A Comparative Study of Two Velocity Profile Models for Rapid Stroke Analysis," *Proceeding of the 16th International Conference on Pattern Recognition*, Quebec, Canada, vol. 4, pp. 52-55, 2002.
- [40] M. Djioua, "Contributions à la généralisation, à la compréhension et à l'utilisation de la théorie cinématique dans l'analyse et la synthèse du mouvement humain," Ph.D. dissertation, Dept. of Electrical, École Polytechnique de Montréal, 2007.
- [41] R. Plamondon, "A kinematic theory of rapid human movements. Part II. Movement time and control," *Biological Cybernetics*, vol. 72, pp. 309-320, 1995.
- [42] R. Plamondon, C. Feng, and A. Woch, "A kinematic theory of rapid human movement. partIV: a formal mathematical proof and new insights," *Biological Cybernetics*, vol. 89, pp. 126-138, 2003.
- [43] D. W. Marquardt "An algorithm for least-squares estimation of non-linear parameters," *Journal of the Society of Industrial and Applied Mathematics*, vol. 11, pp. 431-441, 1963.
- [44] A. Woch and R. Plamondon, "Analysis of movement primitives with the DL model: insights on the age effect," *Proceeding of the 13th Conference of International Graphonomics Society (IGS2007)*, vol. 13, pp. 56-59, 2007.

L'École Polytechnique se spécialise dans la formation d'ingénieurs et la recherche en ingénierie depuis 1873



École Polytechnique de Montréal

**École affiliée à l'Université
de Montréal**

Campus de l'Université de Montréal
C.P. 6079, succ. Centre-ville
Montréal (Québec)
Canada H3C 3A7

www.polymtl.ca

